

Numerical simulation of water droplet behaviors in two novel block channels of PEMFC using dynamic wettability model

Qiaoyu Guo, Mengjie Li, Yanhong Liu, Yu Li, Suihui Ma, Yanzhou Qin *
State Key Laboratory of Engines, Tianjin University, Tianjin, 300350, China

ABSTRACT

Liquid water transport and removal is important in proton exchange membrane fuel cell (PEMFC) for its performance and durability. In this study, we designed two novel channels with different blocks to study their effects on water removal using the Kistler model. Compared with the single straight channel, both of the novel channels can promote droplet removal. The results show that the “one-block” channel leads to a faster water movement and removal, but results in much higher pressure drop. The separated “two-block” channel could achieve both faster water removal and relatively small pressure drop.

Keywords: Water droplet, Dynamic contact angle, Block, Gas diffusion layer, Proton exchange membrane fuel cell

1. INTRODUCTION

Proton exchange membrane fuel cell (PEMFC) is a clean energy conversion device, which directly uses the electrochemical reaction of fuel and oxidant to generate electricity [1]. Recently, baffle block flow channels have been proposed to improve the reactant transport and water removal in the electrode, and have attracted more and more attentions.

Wang et al. [2] designed a new type of channel with trapezoidal baffle plates. They found that the flow fields with the trapezoid baffle plates formed the over-block-convection, which promoted mass transfer from channel to electrode. Yin et al. [3] investigated the influence of the trapezoid baffle block sloping angles on the diffusive oxygen transport and performance of PEMFC. It suggested that when the leading and trailing sloping angles of blocks were 45°, the fuel cell had the best oxygen transport. Although there have been some studies on block channels before, the effect of the block

on liquid water transport in the flow channel is still rare, and its mechanism is not clear. The Kistler model has been applied to the gas diffusion layer (GDL) and the channel wall in the PEMFC to reflect surface dynamic wettability on water behaviors. Andersson et al. [4] found that a dynamic contact angle boundary condition was able to influence the droplet detachment characteristics, such as detachment time and droplet size. Compared with the static contact angle model, the dynamic contact angle model is closer to the real situation.

In this study, a 3D model is established to simulate the droplet movement in flow channels by the volume of fluid (VOF) method. We propose two novel channels with different block designs for water removal, namely one-block channel and two-block channel. The water droplet behaviors in the novel channels are investigated using the dynamic contact angle model.

2. MODEL DESCRIPTION

2.1 Equations and the VOF method

The VOF model is widely used in the study of liquid water. The continuity and momentum equations of the water-air two-phase flow can be expressed, respectively, as:

$$\frac{\partial(\rho)}{\partial t} + \nabla \cdot (\rho \mathbf{V}) = 0 \quad (1)$$

$$\frac{\partial(\rho \mathbf{V})}{\partial t} + \nabla \cdot (\rho \mathbf{V} \mathbf{V}) = -\nabla P + \mu \nabla \cdot (\nabla \mathbf{V} + \nabla \mathbf{V}^T) + \rho \mathbf{g} + \mathbf{F}_s \quad (2)$$

where ρ is the average density (kg m^{-3}), \mathbf{V} is velocity vector (m s^{-1}), P represents static pressure (Pa), μ represents the average viscosity (kg s m^{-2}), and \mathbf{F}_s denotes the source term of surface tension. f_1 and f_2 are the gas phase and the liquid phase volume fraction, respectively, as:

Selection and peer-review under responsibility of the scientific committee of the 12th Int. Conf. on Applied Energy (ICAE2020).

Copyright © 2020 ICAE

$$f_1 + f_2 = 1 \quad (3)$$

If $0 < f_1 < 1$, the cell contains the liquid phase and gas phase. Solving the transport equation of the volume fraction of the liquid water:

$$\frac{\partial f_2}{\partial t} + \nabla \cdot (f_2 \mathbf{v}) = 0 \quad (4)$$

The pressure drop depends on the surface tension coefficient σ_{lg} (N m^{-1}) and phase interface curvature R_1 and R_2 (m).

$$\Delta p = \sigma_{lg} \left(\frac{1}{R_1} - \frac{1}{R_2} \right) \quad (5)$$

where Δp (Pa) is pressure difference on the liquid surface.

$$\mathbf{F}_s = \sigma_{lg} \frac{\rho \kappa \nabla f_1}{0.5(\rho_1 + \rho_2)} \quad (6)$$

$$\mu = f_2 \mu_2 + (1 - f_2) \mu_1 \quad (7)$$

$$\kappa = \nabla \cdot \mathbf{n} = \nabla \cdot [\hat{\mathbf{n}}_w \cos(\theta) + \hat{\mathbf{t}}_w \sin(\theta)] \quad (8)$$

where ρ (kg m^{-3}) is the average density. μ (kg s m^{-2}) represents the average viscosity. κ (m) is the surface curvature of two intersecting interfaces. θ is the contact angle.

2.2 Boundary conditions and Model definition

For this model, the velocity-inlet and pressure-outlet boundary conditions are used. And the velocity profile at the inlet middle line is supposed to be parabolic [5]:

$$u(y) = \frac{3u}{2} \left(1 - \left(\frac{y}{h_1} \right)^2 \right) \quad (9)$$

$$u(z) = \frac{3u}{2} \left(1 - \left(\frac{z}{h_2} \right)^2 \right) \quad (10)$$

where $u(y)$ and $u(z)$ represent the velocity of each inlet cell at the current density. h_1 and h_2 are height and width of the square inlet.

The model is initialized with static contact angle and simulated with dynamic contact angle. The empirical model of Kistler [4] is implemented on the wall:

$$\theta_d = f_{\text{HOFF}}(Ca + f_{\text{HOFF}}^{-1}(\theta_s)) \quad (11)$$

The Hofmann function is defined as:

$$f_{\text{HOFF}}(x) = \arccos \left\{ 1 - 2 \tanh \left[5.16 \left(\frac{x}{1 + 1.31x^{0.99}} \right)^{0.706} \right] \right\} \quad (12)$$

The capillary number Ca represents the ratio of viscous and surface tension forces, and is defined as:

$$Ca = \frac{v\mu}{\sigma} \quad (13)$$

where v is the magnitude of characteristic liquid velocity.

As shown in Fig.1 (a), (b) and (c), the straight channel, one-block channel and two-block channel are described, respectively. The block width of one-block channel is the same as the width of the channel, while the two blocks of two-block channel are separated, and a gap exists between two blocks. The static contact angle of the block and GDL is 80° and 140° , respectively. The values for the parameters mostly agree with the previous research (defined in Table 1) [3].

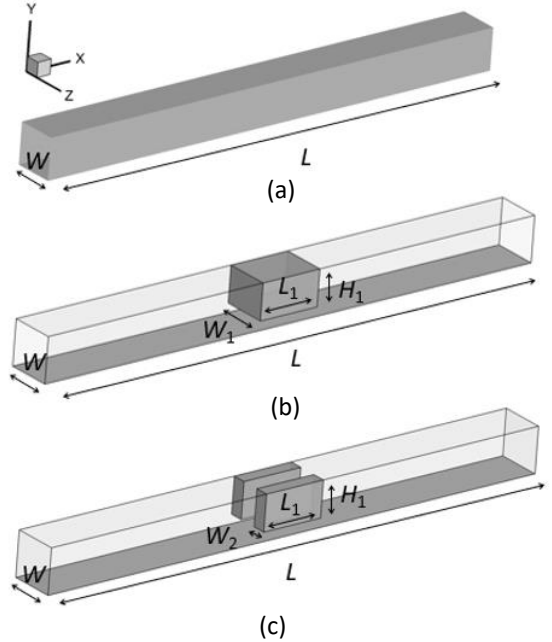


Fig.1 (a) straight channel, (b) one-block channel and (c) two-block channel

Table 1. Model parameters

Parameters	Values
Channel length, L	12 mm
Channel width, W	1 mm
Channel cross section	1 mm X 1 mm
Block length, L_1	1.4 mm
One-block width, W_1	1 mm
Block height, H_1	0.8 mm
Two-block width, W_2	0.3 mm
Density water, ρ_l	998.2 kg m^{-3}
Density air, ρ_g	Volume-weighted-mixing-law
Viscosity air, μ_g	$1.899 \times 10^{-5} \text{ kg s m}^{-1}$
Surface tension, σ_{lg}	0.066 N m^{-1}
Temperature, T	333.15 K
Activation area	3 cm X 3 cm
Droplet radius	0.2 mm

Table 2. Model case

Case	Model	Velocity (m s ⁻¹)
1	Straight channel	5
2	Straight channel	8
3	One-block channel	5
4	One-block channel	8
5	Two-block channel	5
6	Two-block channel	8

3. RESULTS

The water droplet movement is shown in Fig. 2. When the current density is 1 A cm⁻² and 1.6 A cm⁻², the average inlet velocity is 5 m s⁻¹ and 8 m s⁻¹, respectively. As shown in Fig.2 (a) and (b), the droplet flows smoothly in the straight channel. Compared with Fig.2 (c) and (d), it shows that droplet splits out some tiny droplets at the velocity of 8 m s⁻¹ in the one-block channel.

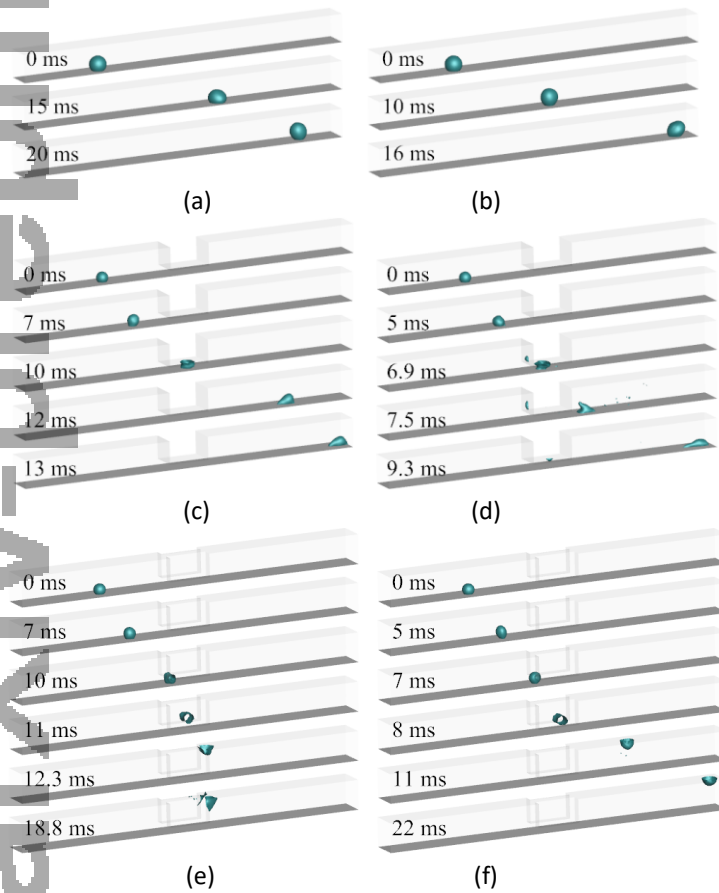
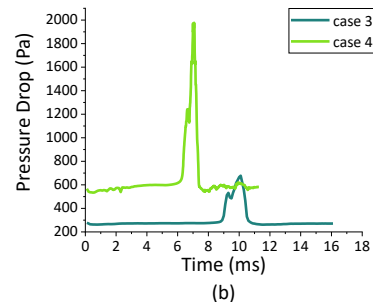
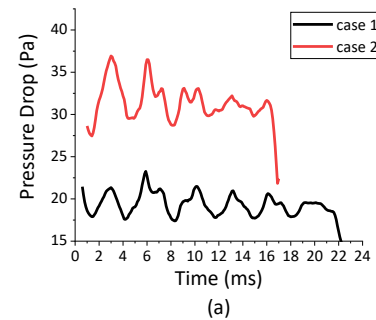


Fig.2 Water droplet shape in the (a) straight channel at the velocity of 5 m s⁻¹, (b) straight channel at the velocity of 8 m s⁻¹, (c) one-block channel at the velocity of 5 m s⁻¹, (d) one-block channel at the velocity of 8 m s⁻¹, (e) two-block channel at the velocity of 5 m s⁻¹ and (f) two-block channel at the velocity of 8 m s⁻¹

This is because the droplet receives a larger shear force at the high air velocity when the droplet passes under the block. Thus, the droplet is more likely to split at the velocity of 8 m s⁻¹. At the high air velocity, a part of the droplet sticks to the wall of the block due to the high speed of droplet and the hydrophilic block in the one-block channel, as shown in Fig.2 (d). In contrast to the straight channel, the structure of the one-block channel helps the droplet flow out of the channel faster. Surprisingly, Fig.2 (e) and (f) show that the droplet rises upwards and leaves the GDL surface when it passes through the gap in the two-block channel. The surface wicking force rises the droplet up. At the velocity of 5 m s⁻¹, since the block surface and the upper wall surface are hydrophilic and the air velocity is low, the droplet accumulates in the corner. At velocity of 8 m s⁻¹, the inertial force of the droplet is greater than the adhesion force, which causes the droplet to pass through the gap smoothly and flow out of the flow channel along the upper surface in the two-block channel. As shown in Fig.2 (f), there is a similar phenomenon to Fig.2 (d) that the droplet also splits out some tiny droplets at 11 ms. In contrast to the one-block channel, the structure of the two-block channel can promote the droplet to leave GDL surface.

Fig.3 shows the instantaneous pressure drop of the three models. As the Fig.3 (a) shows, it is clear that the pressure drop fluctuates within a small range in the straight channel at the velocity of 5 m s⁻¹ and 8 m s⁻¹. However, in the one-block channel and two-block



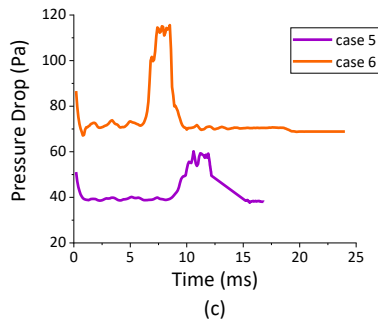


Fig.3 Instantaneous pressure drop of (a) straight channel at the velocity of 5 m s^{-1} and 8 m s^{-1} , (b) one-block channel at the velocity of 5 m s^{-1} and 8 m s^{-1} and (c) two-block channel at the velocity of 5 m s^{-1} and 8 m s^{-1}

channel, the pressure drop increases greatly and has peaks at the velocity of 5 m s^{-1} and 8 m s^{-1} , as shown in Fig.3 (b) and (c). In two block channels, when the droplet passes under the block or passes through the gap, air flow path becomes narrow and so the pressure drop increases during this time. Moreover, the higher the velocity is, the earlier the pressure drop peak occurs and the greater the value of the peak is. And compared to the two-block channel, the structure of the one-block channel results in the higher value of pressure drop due to the larger volume of the block in the channel.

When the droplet flows out of the channel or leaves from the GDL surface, the instantaneous water coverage ratio on the surface of GDL becomes zero. It can be seen from Fig. 4 (a) and (b) that compared to the straight channel, the speed of the droplet is improved so that the droplet leaves the flow channel earlier in the one-block channel. Even better, in the two-block channel the water coverage ratio of 0 occurs earliest compared to other channels because the droplet can rise up in the gap, as shown in Fig.4 (c). Therefore, the two-block channel is more advantageous on water removal.

4. CONCLUSIONS

According to the above simulation, the following important results are obtained: The one-block channel is beneficial to remove droplet by increasing the speed of droplet. And the droplet splits out some tiny droplets at the velocity of 8 m s^{-1} . Meanwhile, when the droplet passes under the block, pressure increases sharply because the air flow path becomes narrow. The two-block channel is useful to remove droplet from the gas diffusion layer (GDL) surface by rising up the droplet. At the velocity of 5 m s^{-1} , the droplet accumulates in the corner of the upper wall. At the velocity of 8 m s^{-1} , the droplet breaks slightly. When the droplet passing through the gap, pressure drop increases, too. However, the pressure peak of the two-block channel is much less

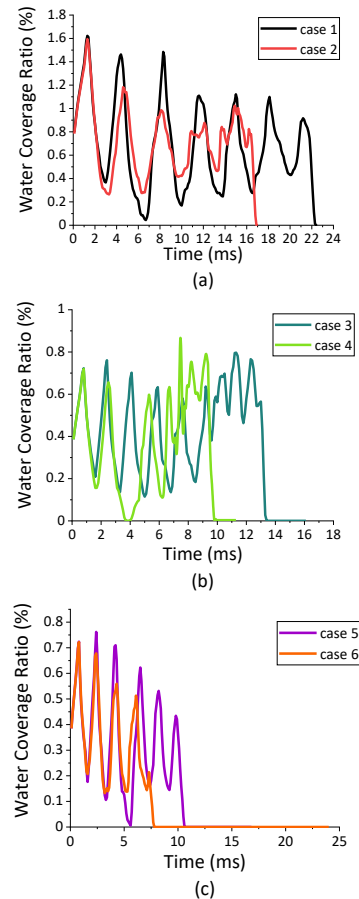


Fig.4 Instantaneous water coverage ratio on the surface of GDL in the (a) straight channel at the velocity of 5 m s^{-1} and 8 m s^{-1} , (b) one-block channel at the velocity of 5 m s^{-1} and 8 m s^{-1} and (c) two-block channel at the velocity of 5 m s^{-1} and 8 m s^{-1}

than that of the one-block channel. The higher the velocity is, the earlier the water is removed, but the greater the value of the pressure drop peak is. Compared to the velocity of 5 m s^{-1} , the pressure drop peak occurs earlier at the velocity of 8 m s^{-1} .

ACKNOWLEDGEMENT

This work is financially supported by the National Natural Science Foundation of China (Grant No. 51706153).

REFERENCE

- [1]Aiyejina A, Sastry MKS. PEMFC Flow Channel Geometry Optimization: A Review. J FUEL CELL SCI TECH. 2012;9.
- [2]Wang X, Qin Y, Wu S, Xiang S, Zhang J, Yin Y. Numerical and experimental investigation of baffle plate arrangement on proton exchange membrane fuel cell performance. J POWER SOURCES. 2020;457
- [3]Yin Y, Wu S, Qin Y, Otoo ON, Zhang J. Quantitative analysis of trapezoid baffle block sloping angles on oxygen transport and performance of proton exchange membrane fuel cell. APPL ENERG. 2020;271.
- [4]Andersson M, Vukcevic V, Zhang S, Qi Y, Jasak H, Beale SB, et al. Modeling of droplet detachment using dynamic contact angles in polymer electrolyte fuel cell gas channels. INT J HYDROGEN ENERG. 2019;44:11088-11096.
- [5]Bahrami M, Yovanovich MM, Culham JR. Pressure drop of fully-developed, laminar flow in microchannels of arbitrary cross-section. 2005. p. 269-280.